Mineralogical Magazine (2021), **85**, 149–160
doi:10.1180/mgm.2020.104

CAMBRIDGE UNIVERSITY PRESS

Article

Spodumene from rare-metal pegmatites of the Kolmozero lithium world-class deposit on the Fennoscandian shield: trace elements and crystal-rich fluid inclusions

Lyudmila N. Morozova[1]*, Ekaterina N. Sokolova[2], Sergey Z. Smirnov[2], Victor V. Balagansky[1] and Aya V. Bazai[1]

[1]Geological Institute of the Kola Science Centre of the Russian Academy of Sciences, 14 Fersman St., Apatity 184209, Russia; and [2]V.S. Sobolev Institute of Geology and Mineralogy of the Siberian Branch of the Russian Academy of Sciences, 3 Akademika Koptyuga Ave., Novosibirsk 630090, Russia

Abstract

The paper investigates trace elements and crystal-rich fluid inclusions in spodumene from rare-metal pegmatites of the Kolmozero lithium deposit in the Kola region, Russia. The main lithium mineral in the pegmatites is spodumene, which occurs in three generations, designated as Spd-I, Spd-II and Spd-III. Iron, Na and Mn are the most typical element impurities in spodumene. The Fe/Mn ratio is 7.1 in Spd-I, 12.3 in Spd-II and 13.2 in Spd-III. Spd-II contains fluid and crystal-rich fluid inclusions. The crystal-rich fluid inclusions in Spd-II originally trapped CO_2-bearing aqueous fluids with dissolved alkali carbonates. The crystal-rich fluid inclusions contain zabuyelite (Li_2CO_3) and cristobalite (SiO_2) as solid phases, which have not been reported previously from the Kolmozero rare-metal pegmatites. These minerals are assumed to have resulted from a reaction between a CO_2-bearing aqueous fluid and host Spd-II and are not related to the mineral-forming system of pegmatites.

Keywords: albite–spodumene pegmatites, spodumene, trace elements, cristobalite, zabuyelite, inclusions, Kolmozero lithium deposit, Kola region, Fennoscandian shield

(Received 19 June 2020; accepted 18 December 2020; Accepted Manuscript published online: 28 December 2020; Associate Editor: Edward Sturgis Grew)

Introduction

The nature and properties of spodumene pegmatite-forming systems are still hotly debated. The overwhelming majority of studies of pegmatite-forming systems have focused on inclusions in quartz, whereas inclusions in spodumene, which is the main lithium mineral in albite–spodumene pegmatites, have received much less attention, with reports in only a limited number of publications (Bazarov, 1976; London, 1986a, 1986b; Zagorsky *et al.*, 1992; Anderson *et al.*, 2001; Li and Chou, 2017; Thomas *et al.*, 2011; Anderson, 2013, 2019). Trace elements in spodumene have been considered by Fersman (1960), Ginzburg (1959), Gordienko (1996), Černý and Ferguson (1972). Investigations of trace elements and inclusions in albite–spodumene pegmatites significantly expand our understanding of the genesis of these rocks. The relevance of these investigations is highlighted by the fact that albite–spodumene pegmatites represent one of the primary sources of lithium, which is essential for the high-tech industries (Černý, 1982; Černý and Ercit, 2005; Kesler *et al.*, 2012; London, 2017; Bowell *et al.*, 2020). This research provides the first data on trace elements and composition of inclusions in spodumene from rare-metal pegmatites of the Kolmozero lithium deposit in the Kola region in the northeastern Fennoscandian shield and is the largest lithium deposit in Russia (Bykhovsky and Arkhipov, 2016).

*Author for correspondence: Lyudmila N. Morozova, Email: morozova@geoksc.apatity.ru
Cite this article: Morozova L.N., Sokolova E.N., Smirnov S.Z., Balagansky V.V. and Bazai A.V. (2021) Spodumene from rare-metal pegmatites of the Kolmozero lithium world-class deposit on the Fennoscandian shield: trace elements and crystal-rich fluid inclusions. *Mineralogical Magazine* **85**, 149–160. https://doi.org/10.1180/mgm.2020.104

Geological setting

Regional geology

Albite–spodumene pegmatites of the Kolmozero lithium deposit belong to the Kolmozero pegmatite field (Gordienko, 1970) that occurs in the junction zone of the Archaean Kola and Murmansk provinces (Figs 1, 2). This junction zone has been long considered as an Archaean linear mobile-permeable zone (deep-seated fault), which was activated partially in the Palaeoproterozoic (Kratz, 1978; Rundqvist and Mitrofanov, 1993). This tectonic structure is now interpreted as the Archaean Kolmozero–Voron'ya greenstone belt transformed into an Archaean accretionary orogen, which can also be classified as an imbricated suture zone (Mints, 2015a). From the view point of modern structural geology, we interpret high-strain zones around, and within this suture, as transcrustal shear zones. Due to their high permeability, these zones are channels for circulating ore-bearing fluids that yield ore mineralisation in the zones and their walls (McCaffrey *et al.*, 1999). Fractures can also be structures conducive to ore mineralisation, though the long-term exploration of the Kolmozero lithium pegmatites and our studies have not discovered any fractures of this type.

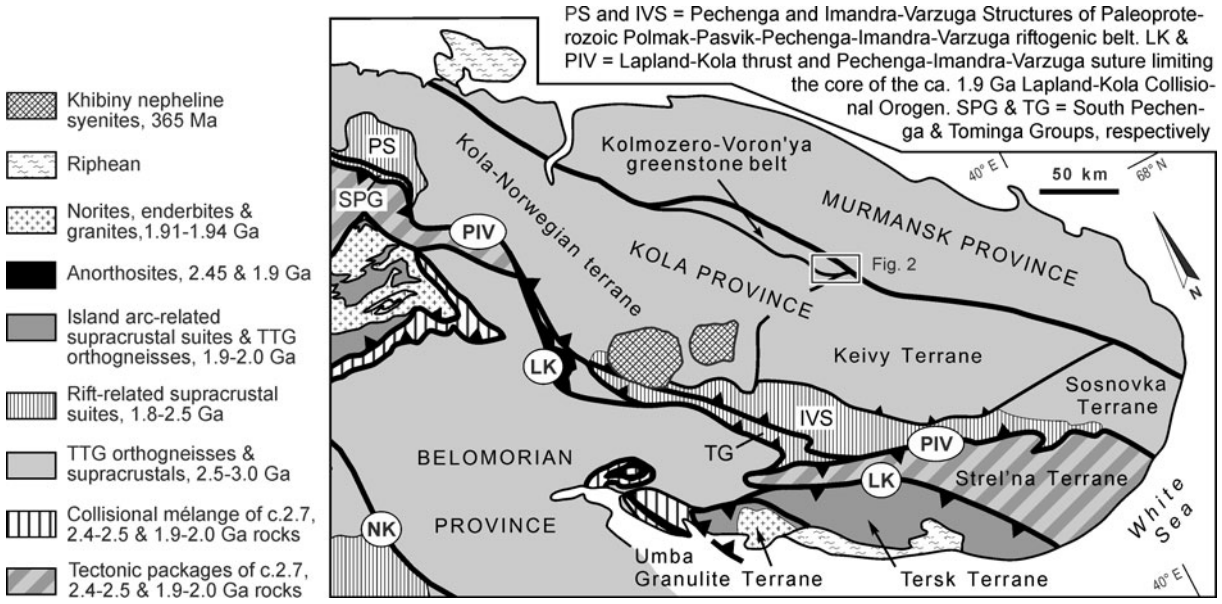

Fig. 1. Tectonic provinces of the northeastern part of the Fennoscandian shield (modified from Daly *et al.*, 2006).

The continental crust of the Murmansk and Kola provinces was formed and underwent major metamorphic and deformational reworking 2.6–2.9 Ga ago (Timmerman and Daly, 1995; Kozlov *et al.*, 2006; Hölttä *et al.*, 2008; Mints, 2015b). The Murmansk province is composed principally of late Mesoarchaean and Neoarchaean granites, enderbites, charnockites and tonalite–trondhjemite gneisses with relics of supracrustal rocks (Vetrin, 1984; Rundqvist and Mitrofanov, 1993; Mints, 2015b). These rocks underwent high-temperature amphibolite-facies metamorphism and locally contain relics of granulite-facies mineral assemblages (Petrov *et al.*, 1990; Mints, 2015b). The Kola–Norwegian, Keivy and Kolmozero–Voron'ya terranes represent the main tectonic units of the Kola province (Daly *et al.*, 2006). The Kola–Norwegian and Keivy terranes are generally made up of tonalite–trondhjemite–granodiorite gneisses, charnockites and enderbites, metasediments and subordinate amphibolites. The Kolmozero–Voron'ya terrane is composed principally of metabasalts, metakomatiites, intermediate and felsic volcanic rocks and subordinate metasedimentary rocks of the late Mesoarchaean Kolmozero–Voron'ya greenstone belt, which is also known as the Polmos–Poros belt (Rundqvist and Mitrofanov, 1993; Glebovitsky, 2005). The greenstone rocks underwent amphibolite-facies metamorphism (Petrov *et al.*, 1990).

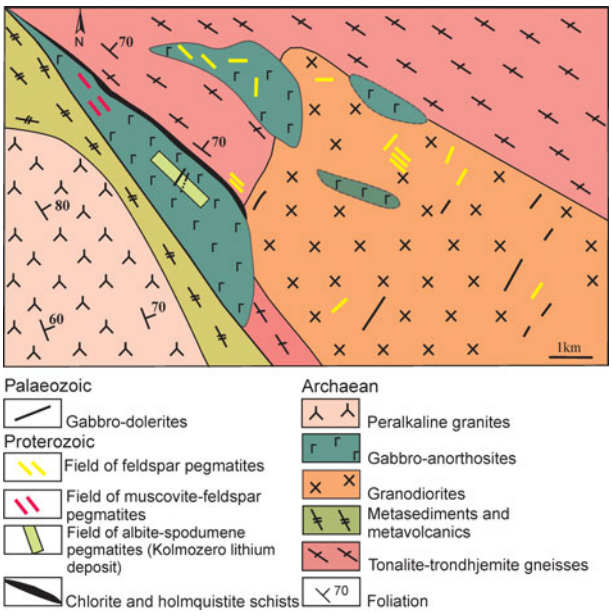

Fig. 2. Schematic geological map of the Kolmozero pegmatite field (modified from Morozova, 2018, figure 2).

The main tectonic boundaries of northern Fennoscandia finally formed in the Palaeoproterozoic during the Lapland–Kola collisional orogeny (Daly *et al.*, 2006; Hölttä *et al.*, 2008; Lahtinen and Huhma, 2019). The history of the Lapland–Kola collisional orogen includes intracontinental rifting of Archaean crust (2.5–2.1 Ga), Red Sea-type oceanic separation (~2.1–2.0 Ga), subduction and crustal growth (~2.0–1.9 Ga), intercontinental collision (1.94–1.86 Ga) and orogenic collapse and exhumation (1.90–1.86 Ga). The Kola province was the northeastern foreland of the Lapland–Kola orogen and experienced Palaeoproterozoic deformational reworking predominantly along boundaries of main tectonic structures, whereas the Murmansk province is essentially free of Palaeoproterozoic deformation (Daly *et al.*, 2006).

Kolmozero pegmatite field

The Kolmozero pegmatite field is entirely within the Murmansk province (Figs 1, 2; Gordienko, 1970). This pegmatite field occurs in Archaean tonalite–trondhjemite gneisses that are intruded by the Kolmozero massif of metagabbrodiorites, metamonzodiorites and metagranodiorites of sanukitoid affinities of 2.73 Ga (Kudryashov *et al.*, 2013) and gabbro–anorthosites of the Patchemvarek massif of 2.66 Ga (Vrevsky and Lvov, 2016) and its two satellites, the Severny and Bezymyanny massifs.

On the basis of mineralogical and structural characteristics, albite–spodumene, muscovite–feldspar and feldspar pegmatites have been distinguished (Gordienko, 1970; Morozova, 2018).

Cross-cutting relationships between these different pegmatites have remained unclear. The albite–spodumene pegmatites contain spodumene in sufficient quantities to be economic and constitute the Kolmozero lithium deposit that also has Be, Ta and Nb mineralisation. The ore-bearing pegmatites intrude the Patchemvarek metagabbros–anorthosites that forms a steeply northeastwardly dipping lenticular massif up to 2 km thick and ~7 km across. Along the massif margins metagabbro–anorthosites are sheared and transformed into fine-grained amphibolites, which indicate a tectonic origin of the massif boundaries. The muscovite–feldspar pegmatites contain Be–Nb–Ta mineralisation and intrude metagabbros–anorthosites of the Bezymyanny massif. The feldspar pegmatites have only Be mineralisation and are widespread north of the Kolmozero lithium deposit in the rocks of the Kolmozero and Severny gabbro–anorthosite massifs and tonalite–trondhjemite gneisses.

Chlorite and holmquistite schists that occur along the northern boundary of the Patchemvarek metagabbros–anorthosite massif with tonalite–trondhjemite gneisses are interpreted as a metasomatic reworking of metagabbro–anorthosites during the pegmatite formation (Gordienko, 1970). The pegmatites are located in a northwest-trending shear zone along which metasomatic fluids circulated. Metasomatic halos have not been found around pegmatite veins.

Methods

Silica and alumina concentrations in spodumene were determined using a Cameca MS-46 microprobe operated in a wavelength-dispersive spectroscopy mode at 22 kV and 20–40 nA. Reference standards were wollastonite (Si*K*α) and $Y_3Al_5O_{12}$ (Al*K*α) at the Geological Institute of the Kola Science Centre of the Russian Academy Sciences (Apatity, Russia).

Contents of minor and trace elements in spodumene were determined by laser ablation inductively coupled plasma mass spectrometry (LA-ICP-MS) using a NexION 300S (PerkinElmer) quadruple inductively coupled plasma mass-spectrometer with a NWR 213 laser ablation instrument at the Geoanalitik Core Facilities Centre of the Institute of Geology and Geochemistry of the Urals Branch of the Russian Academy of Sciences (Yekaterinburg, Russia). The analysis was carried out at an ISO class 7 clean room. Laser ablation was performed at pulse repetition rate 12 Hz and laser energy density 10.5–11.5 J/cm^2 in a spot (crater diameter) 50 μm in size. The results were processed using *GLITTER V4.4* software (GEMOC, Macquarie University, Australia) and an internal SiO_2 standard. NIST SRM 610 glass was measured as the primary external standard after each 10–12 analyses of spodumene. NIST SRM 612 glass was used as the secondary standard. Concentrations were determined for the following elements: Li, Be, B, Na, Mg, Ca, Sc, Ti, V, Cr, Fe, Mn, Co, Ni, Cu, Zn, Ga, Ge, As, Se, Rb, Sr, Y, Zr, Nb, Mo, Ag, Cd, In, Sn, Sb, Te, Cs, Ba, La, Ce, Pr, Nd, Sm, Eu, Gd, Tb, Dy, Ho, Er, Tm, Yb, Lu, Hf, Ta, W, Tl, Pb, Bi, Th and U.

Inclusions in spodumene and quartz were studied at the Fluid Inclusion Laboratory and Core Facilities Centre for multi-element and isotope research of the V.S. Sobolev Institute of Geology and Mineralogy of the Siberian Branch of the Russian Academy of Sciences (IGM SB RAS) (Novosibirsk, Russia). The inclusions were investigated in sections polished on both sides. Optical microscopy of inclusions in quartz and spodumene was performed using an Olympus BX-51 microscope with an Infinity photo camera.

The identification of mineral phases in the crystalline aggregate of crystal-rich fluid inclusions were performed using Tescan Mira 3 LMU and LEO-1430VP scanning electron microscopes (IGM SB RAS), and by Raman spectroscopy using a Horiba LabRam HR 800 spectrometer with a semiconductor detector (IGM SB RAS).

The microthermometric investigation of crystal-rich fluid inclusions in spodumene and fluid inclusions in quartz within a temperature range of –180 to +600°C was made using a Linkam THMSG600 heating–freezing stage (IGM SB RAS). The accuracy at low temperatures (<0°C) is 0.1°C; however, due to the small size of the inclusions (5–15 μm), the errors of determination of the eutectic point, ice melting and homogenisation are as high as a few degrees. The gas–phase composition and some crystalline phases in fluid and crystal-rich fluid inclusions were determined using a Horiba Lab Ram HR 800 Raman spectrometer. The spectra were excited by a solid-state 532 nm Nd YAG laser with output power of 50 mW. The spectrum was taken by a Peltier cooled Endor semiconductor detector with working temperature –70°C. A confocal optical system based on an OLYMPUS BX-41 microscope with a LNA 100× objective was used for focusing the laser to the object studied and collection of the scattered beam. The acquisition time and size of the confocal pinhole varied depending on the size of the analysed phase.

Kolmozero lithium deposit

Geological structure and geochemistry of pegmatite

The Kolmozero lithium deposit consists of 12 large northwest-trending, steeply southwestwardly dipping ore-bearing veins of albite–spodumene pegmatite, as well as numerous small veins with apophyses (Figs 3a,b). The large veins have lengths of over 1400 m and thicknesses of 5 to 65 m and extend down to depths of >500 m. The albite–spodumene pegmatites are cross-cut by Palaeozoic (?) gabbro–dolerite dykes. The pegmatite veins have sheet-like morphology and display no prominent concentric zoning. A quartz–plagioclase aplite up to 5 cm in thickness and coarse-grained quartz–albite aggregates to 30 cm thick were observed at the contact with the country rocks. The veins (85–90%) are almost entirely composed of the coarse- and very coarse-grained quartz–spodumene–feldspar pegmatite. This pegmatite contains segregations of blocky microcline, granular quartz and cleavelandite, quartz–albite aggregates, quartz–muscovite veinlets, saccharoidal albite veinlets, and clusters of beryl and columbite-group minerals. Greyish-pink microcline–perthite (Mc-I) forms rare crystals up to 10 cm in size and aggregates of blocky dark-pink microcline (Mc-II) up to 40–60 cm in size compose separated areas 5 m × 2 m within veins. A quartz core has been found in only one vein by drilling (Gordienko, 1970).

The major pegmatite minerals are: quartz (30–35 vol.%); albite (30–35 vol.%); microcline (10–25% vol.%); spodumene, the main lithium mineral (~20% vol.%); and muscovite (5–7 vol.%). Accessory beryl and columbite-group minerals which might have economic interest as a source of Be, Ta and Nb if sufficiently abundant occur in the very large veins. Other accessory minerals include: spessartine; apatite; rare lithiophilite ($LiMnPO_4$); triphylite ($LiFePO_4$); and tourmaline. Tourmaline is a typical minor mineral in other rare-metal pegmatites of the northeastern Kola region and its occurrence as a rare accessory mineral is a characteristic feature of the Kolmozero rare-metal pegmatite. Biotite occurs at contacts with the metagabbros–anorthosite host rock.

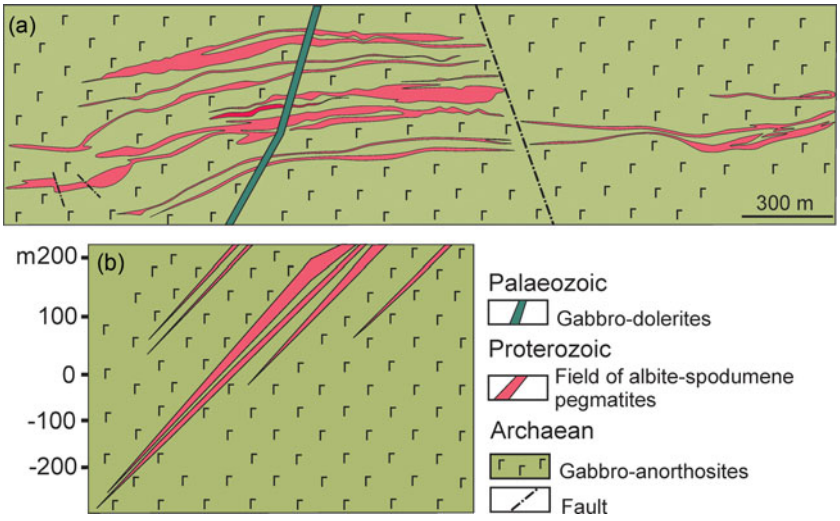

Fig. 3. (a) Schematic geological map of the Kolmozero lithium deposit. (b) Cross-section illustrating depths of the occurrence of albite–spodumene pegmatites (modified from Morozova, 2018, figure 3).

Phosphates and zeolites predominate among secondary minerals. Sixty four mineral species have been recognised in the Kolmozero albite–spodumene pegmatites (Gordienko, 1970).

Spodumene is the main carrier of Li_2O in the Kolmozero deposit with 97 wt.% of the total, 0.3 wt.% is carried by lithiophilite and 0.45 wt.% by muscovite (Gordienko, 1970).

The albite–spodumene pegmatites are enriched in: (ppm) Cs (23); Nb (81); Ta (59); Be (142); and Li (12,244). In the albite–spodumene pegmatites the amount of rare earth elements (REE) is ≤3 ppm. These rocks are depleted (ppm) in: Ba (≤20); Sr (≤15.4); Y (≤0.46); Th (≤2.5); and Zr (≤22). They demonstrate low fractionation indexes for Mg/Li ≤0.05 and Zr/Hf ≤7.4 (Morozova, 2018, 2019). Rare-metal lithium–caesium–tantalum (LCT) pegmatites from other regions of the world have similar geochemical features (Chachowsky, 1987; Černý, 1991, 1992; Lagache, 1997; Černý and Ercit, 2005; Zhu *et al.*, 2006; London, 2008).

A U–Pb radiometric age of 2315 ± 10 Ma for columbite-(Mn) from an albite–spodumene pegmatite is interpreted to give an age for the rare-metal mineralisation (Morozova *et al.*, 2017). This age indicates that the albite–spodumene pegmatites formed during the early Palaeoproterozoic rifting of the Fennoscandian shield (Hanski and Melezhik, 2013).

Spodumene samples

In the Kolmozero albite–spodumene pegmatites spodumene belongs to three morphological types or generations: spodumene-I (Spd-I); spodumene-II (Spd-II); and spodumene-III (Spd-III) occurring in central parts of the veins (Gordienko, 1970; Morozova and Bazai, 2019). Spd-I is represented by opaque, greyish-green prismatic crystals up to 10 cm long. Polarised-light microscopic observations reveal two systems of cleavage planes at an angle of 87° and {100} twins. Spd-I occurs in coarse-grained quartz–spodumene–albite aggregates and is replaced by saccharoidal albite at crystal margins (Fig. 4b). Mineral inclusions in Spd-I are: albite; quartz; muscovite; microcline; and columbite-group minerals. Spd-I crystallised before blocky Mc-II, cleavelandite and large sheets of muscovite (up to 10 cm long), and after Mc-I (Gordienko, 1970).

Spd-II occurs as long-to-short prismatic lath-shaped crystals, either individually or aggregated (blocky spodumene), in association with coarse- and very coarse-grained albite and quartz. The crystals are opaque, rarely semi-transparent, greyish-green and green. Individual crystals can reach up to 1.5 m in length. Microscopic investigation reveals twins parallel to {100} (Figs 4a,c). Spd-II contents are high, which makes the albite–spodumene pegmatites a lithium ore. Spd-II contains micro-inclusions of: albite; quartz; muscovite; apatite; cassiterite; and columbite-group minerals. Spd-II crystallised simultaneously with blocky Mc-II prior to cleavelandite and large sheets of muscovite (Gordienko, 1970).

Spd-III was identified in thin sections in fine-grained quartz–muscovite–spodumene–albite aggregate (Fig. 4d). The mineral occurs as short prismatic and equant crystals up to 0.5 mm in size. The Spd-III crystals, and the aggregates, fill cracks at margins of the Spd-II crystals.

Results

Geochemistry of spodumene

Spodumene, $LiAl(Si_2O_6)$, is a clinopyroxene. The structure is composed of chains of SiO_4 tetrahedra, running along the *c* axis and connected by Al^{3+} (*M*1) and Li^{+} (*M*2) cations (Deer *et al.*, 1978). Representative compositions of the spodumene from the Kolmozero deposit are given in Tables 1, 2 and Fig. 5. Lithium contents were determined by LA-ICP-MS and by stoichiometric calculations using electron microprobe data. The LA-ICP-MS values are consistently higher than those calculated from stoichiometry, which we attribute to processing of the extremely high signal intensities resulting from the LA-ICP-MS analytical procedure. Thus, our formula calculations are based on Li contents determined by stoichiometry. Structural formulae of the spodumene were calculated on the basis of six oxygen atoms and the total cation charge proved to be 12.00, i.e. the charge-balance is met and the mineral formulae are close to ideal, $LiAlSi_2O_6$ (Table 1).

In addition to Li, Al and Si, spodumene contains minor elements among which Fe, Mn and Na dominate. The mass fraction of these elements of the total minor and trace-element contents is 94% in Spd-I and 97% in Spd-II and Spd-III. Spd-I differs from Spd-II and Spd-III in having higher Mn (773 ppm *vs.* 657 and 665 ppm, respectively). These differences are reflected in the Fe/Mn ratio which is 7.1 in Spd-I and 12.3 and 13.2 in Spd-II and Spd-III, respectively. The Na contents in Spd-I and Spd-II are almost identical (1159 and 1119 ppm, respectively), whereas

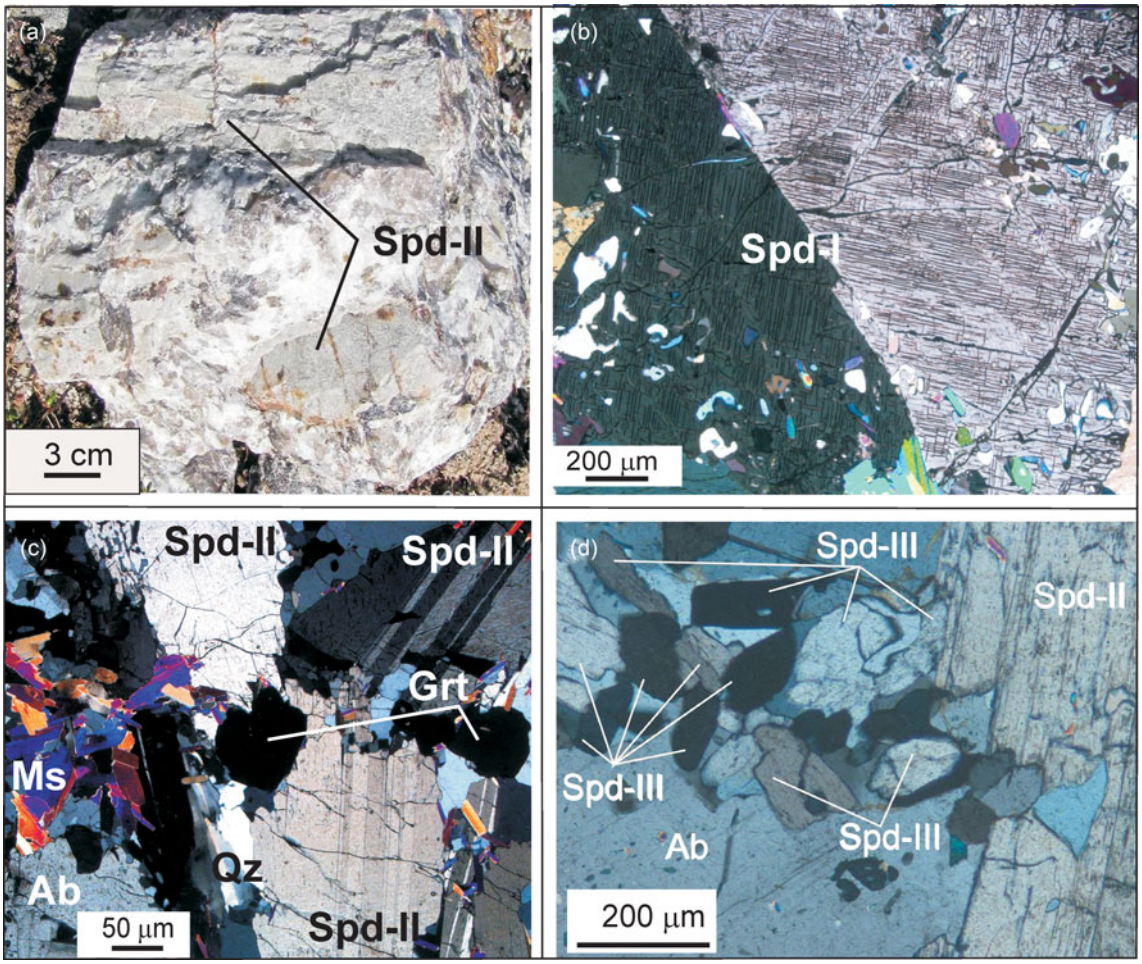

Fig. 4. (a) Photograph of hand specimen and (b–d) photomicrographs of thin sections of albite–spodumene pegmatites (crossed polarised light). Ab, albite; Gr, garnet; Ms, muscovite; Qz, quartz; Spd, spodumene.

Table 1. Representative compositions (wt.%) for the Kolmozero spodumenes.

Type		Spd-I			Spd-II			Spd-III		
Sample no.		#Kl-9	#Kl-8/2a	#Kl-8/2a	#Kl-23	#Kl-11/2	#Kl-23a	#Kl-23	#Kl-11/2-	#Kl-23
$SiO_2^{‡}$		64.43	64.56	64.56	64.55	64.57	64.55	64.50	64.53	64.50
$Al_2O_3^{‡}$		26.79	26.97	26.97	26.92	26.95	26.95	26.82	26.87	26.82
$Fe_2O_3^{‡}$		0.76	0.75	0.83	1.06	1.21	1.13	1.19	1.32	1.20
$MnO^{†}$		0.09	0.11	0.10	0.08	0.10	0.07	0.09	0.10	0.07
$Na_2O^{†}$		0.15	0.17	0.16	0.14	0.15	0.16	0.21	0.18	0.20
$Rb_2O^{†}$		0.01	n.d.	n.d.	n.d.	n.d.	n.d.	n.d.	n.d.	n.d.
Li_2O^{*}		7.94	7.96	7.97	7.98	7.99	7.97	7.94	7.97	7.94
Total		100.16	100.51	100.59	100.73	100.97	100.83	100.75	100.97	100.73
Li_2O^{**}		7.95	8.14	8.21	8.22	8.79	8.10	8.22	8.90	8.62
Formula calculated on the basis of 6 apfu										
T	Si^{4+}	2.001	1.998	1.997	1.995	1.995	1.994	1.995	1.993	1.995
*M*1	Al^{3+}	0.980	0.983	0.983	0.980	0.980	0.981	0.977	0.978	0.977
	Fe^{3+}	0.018	0.017	0.019	0.025	0.028	0.026	0.028	0.031	0.028
	Mn^{2+}	0.002	0.003	0.003	0.002	0.003	0.002	0.002	0.003	0.002
Σ *M*1		1.000	1.004	1.005	1.007	1.011	1.009	1.008	1.011	1.007
*M*2	Na^{+}	0.009	0.010	0.009	0.008	0.009	0.010	0.013	0.011	0.012
	Rb^{+}	0.000								
	Li^{+}	0.991	0.990	0.991	0.992	0.991	0.990	0.987	0.989	0.988
Σ *M*2		1.000	1.000	1.000	1.000	1.000	1.000	1.000	1.000	1.000
Σ Cat		4.001	4.002	4.002	4.002	4.006	4.003	4.002	4.003	4.002

‡ Determined by EMPA; † Determined by LA-ICP-MS; * Calculated from stoichiometry; ** Calculated from LA-ICP-MS data; n.d., not detected.
Tabulated Li contents per formula unit were calculated from stoichiometry.

Table 2. Trace elements in the Kolmozero spodumenes (ppm).

Sample no	Spd-I #Kl-9	#Kl-8/2a	#Kl-8/2a	average	Spd-II #Kl-23	#Kl-11/2	#Kl-23a	average	Spd-III #Kl-23	#Kl-11/2	#Kl-23	average
Ti	72.17	96.02	114.99	94.39	54.68	57.88	58.06	56.87	47.43	64.51	60.06	57.33
Mg	27.36	17.61	22.44	22.47	26.56	33.87	14.7	25.04	29.77	30.53	23.68	27.99
Ga	107.89	87.25	74.78	89.97	69.62	82.74	66.81	73.06	65.36	61.20	61.43	62.66
Ge	9.47	12.22	10.43	10.71	5.33	4.36	9.08	6.26	5.94	4.56	3.99	4.83
Sn	52.46	53.29	116.14	73.96	17.31	39.46	21.5	26.09	21.49	27.38	18.35	22.41
Cu	132.85	129.21	89.59	117.22	69.34	27.27	66.09	54.23	37.52	22.40	53.18	37.70
Rb	105.41	0.39	0.71	35.50	n.d.	n.d.	n.d.	n.d.	n.d.	n.d.	n.d.	n.d.
Ca	n.d.	n.d.	n.d.	n.d.	n.d.	n.d.	n.d.	n.d.	127.64	n.d.	124.16	125.90
Cs	2.08	n.d.	0.18	1.13	0.07	n.d.	0.03	0.05	n.d.	n.d.	0.22	0.22
Be	n.d.	n.d.	3.78	3.78	n.d.	n.d.	n.d.	n.d.	n.d.	n.d.	2.42	2.42
B	7.36	4.46	4.85	5.56	n.d.	3.07	n.d.	3.07	n.d.	n.d.	2.96	2.96
Sc	0.71	n.d.	1.07	0.89	n.d.	0.61	0.65	0.63	n.d.	n.d.	0.70	0.70
V	n.d.	n.d.	n.d.	n.d.	4.62	2.14	3.35	3.37	2.77	2.84	3.33	2.98
Cr	5.49	n.d.	n.d.	5.49	9.81	3.78	4.94	6.18	12.64	n.d.	4.91	8.78
Co	n.d.	n.d.	n.d.	n.d.	n.d.	n.d.	0.26	0.26	0.56	n.d.	n.d.	0.56
Zn	2.69	n.d.	2.80	2.75	3.08	4.65	9.43	5.72	8.91	14.78	10.32	11.34
As	3.97	3.05	3.60	3.54	n.d.	2.34	n.d.	2.34	n.d.	1.77	n.d.	1.77
Se	n.d.	n.d.	n.d.	n.d.	n.d.	20.32	n.d.	20.32	n.d.	19.43	n.d.	19.43
Sr	0.41	n.d.	n.d.	0.41	n.d.	n.d.	n.d.	n.d.	n.d.	n.d.	1.11	1.11
Y	n.d.	n.d.	n.d.	n.d.	0.1	n.d.	n.d.	0.10	n.d.	n.d.	n.d.	n.d.
Zr	n.d.	n.d.	0.45	0.45	n.d.	0.23	n.d.	0.23	n.d.	n.d.	n.d.	n.d.
Nb	3.16	0.13	0.12	1.14	n.d.	n.d.	0.10	0.10	n.d.	0.22	0.06	0.14
Mo	n.d.	n.d.	n.d.	n.d.	n.d.	0.57	n.d.	0.57	n.d.	n.d.	1.26	1.26
Ag	n.d.	n.d.	n.d.	n.d.	n.d.	n.d.	n.d.	n.d.	n.d.	0.17	n.d.	0.17
Cd	3.77	1.79	5.68	3.75	1.12	2.70	0.50	1.44	1.14	1.01	1.19	1.11
In	0.15	0.12	0.55	0.27	n.d.	0.20	0.09	0.15	n.d.	0.22	0.06	0.14
Sb	0.37	0.26	0.14	0.26	n.d.	n.d.	n.d.	n.d.	n.d.	n.d.	n.d.	n.d.
Cs	2.08	n.d.	0.18	1.13	0.07	n.d.	0.03	0.05	n.d.	n.d.	0.22	0.22
Ba	0.19	0.20	0.21	0.20	n.d.	n.d.	n.d.	n.d.	n.d.	n.d.	n.d.	n.d.
La	n.d.	n.d.	n.d.	n.d.	n.d.	n.d.	n.d.	n.d.	n.d.	n.d.	0.05	0.05
Ce	n.d.	0.03	n.d.	0.03	n.d.	n.d.	n.d.	n.d.	n.d.	n.d.	0.05	0.05
Pr	n.d.	n.d.	0.03	0.03	n.d.	n.d.	n.d.	n.d.	n.d.	n.d.	0.02	0.02
Er	n.d.	n.d.	n.d.	n.d.	0.12	n.d.	n.d.	0.12	n.d.	n.d.	n.d.	n.d.
Hf	0.08	0.49	0.18	0.25	n.d.	n.d.	n.d.	n.d.	n.d.	n.d.	n.d.	n.d.
Ta	2.63	0.27	0.15	1.02	n.d.	0.08	0.14	n.d.	n.d.	n.d.	0.03	0.03
Tl	0.31	n.d.	n.d.	0.31	n.d.	0.04	n.d.	0.04	n.d.	n.d.	n.d.	n.d.
Pb	0.16	n.d.	0.04	0.10	0.04	n.d.	n.d.	0.04	n.d.	n.d.	0.23	0.23
Bi	0.03	n.d.	0.12	0.08	n.d.	n.d.	n.d.	n.d.	n.d.	n.d.	n.d.	n.d.
Th	n.d.	n.d.	n.d.	n.d.	n.d.	n.d.	n.d.	n.d.	n.d.	n.d.	0.13	0.13
U	n.d.	n.d.	n.d.	n.d.	n.d.	n.d.	n.d.	n.d.	n.d.	n.d.	0.39	0.39
Fe/Mn	7.16	6.40	7.62	7.06	11.50	10.67	14.70	12.29	12.35	12.04	15.16	13.18

n.d. – not detected; data obtained by the LA-ICP-MS method.

Spd-III is enriched in Na (1475 ppm) compared to Spd-I and Spd-II (Fig. 5).

Inclusions in Spd-II and quartz

A greenish crystal of Spd-II from the central part of an albite–spodumene pegmatite vein was selected for inclusion study. The core of this crystal is turbid, whereas margins are transparent and one marginal domain is cross-cut by a 0.5 mm thick quartz–muscovite veinlet. Polished thin section KL-GX-11b was prepared from this marginal domain. The surface of the section is oriented parallel to the *c* axis of the spodumene crystal, close to the parting plane {100}. Fluid inclusions were studied in both spodumene and quartz.

This Spd-II contains numerous negative crystal-rich fluid inclusions 5–15 μm in size elongated along the *c* axis of the host mineral. The majority of crystal-rich fluid inclusions are distributed irregularly in the host mineral. Commonly, they are arranged along the crossing planes (Fig. 6). The irregularly distributed crystal-rich fluid inclusions are considered as primary. The origin of those confined to crossing planes is not so obvious. The linearly arranged inclusions have an appearance of inclusions trapped along fractures. However, their oblique orientation to the cleavage and parting fractures indicate that they might have other origins. Similar arrangements of inclusions in spodumene were reported by Anderson (2013, 2019) who interpreted them as healed microfractures. The linearly arranged crystal-rich fluid inclusion groups in the spodumene crystal investigated do not cross its outlines and thus could be interpreted as microfractures of unknown nature, healed during the crystal growth, however here they are nonetheless regarded as pseudo-secondary inclusions. Their phase compositions are similar to those interpreted as primary inclusions. Therefore, we believe that the pseudo-secondary inclusions are related genetically to the primary ones and hereafter are considered together.

At room temperature, crystal-rich fluid inclusions contain solid phases, liquid and a gas bubble. Relations between these phases vary significantly and the solid phase abundance and composition is not constant. Crystals within crystal-rich fluid inclusions are most commonly transparent, colourless, euhedral and in some inclusions consist of aggregates of grains. Zabuyelite (Li_2CO_3), cristobalite (SiO_2), an unidentified phyllosilicate, which could be either a mica, chlorite or a clay mineral,

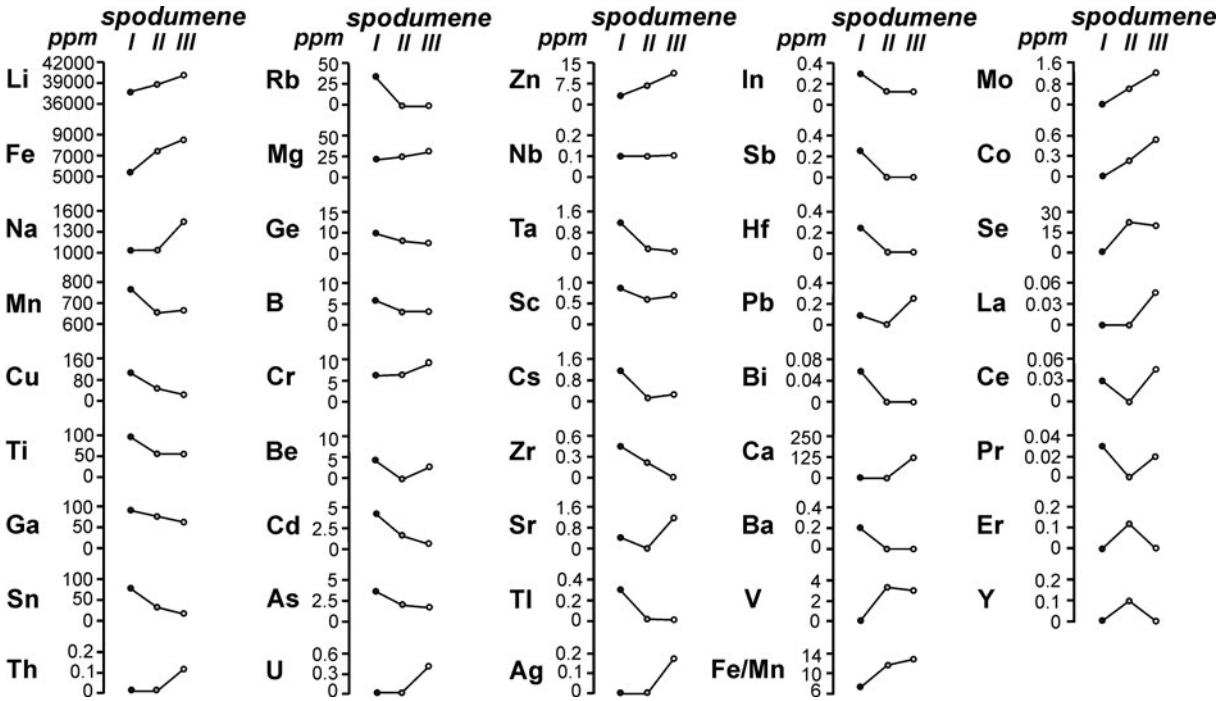

Fig. 5. Concentrations of major, minor and trace elements in the Kolmozero spodumenes; I, II and III spodumene generations.

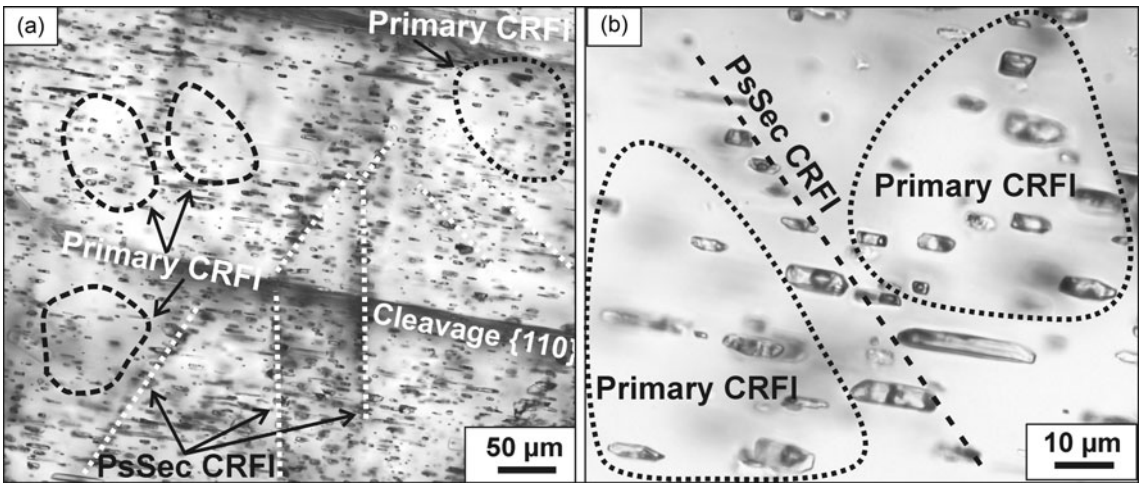

Fig. 6. Photomicrographs (plane polarised light) of typical crystal-rich inclusions in Spd-II. (a) Fissures of cleavage {110} are intersected by planar arrays of pseudosecondary crystal-rich fluid inclusions (PsSec CRFI). Primary crystal-rich fluid inclusions are distributed irregularly in the host mineral. (b) Primary and pseudosecondary CRFI with different proportions of gas, liquid and solid phases.

and locally calcite were identified as solid phases by Raman spectroscopy and scanning electron microscopy energy dispersive analysis (Figs 7, 8). Zabuyelite and cristobalite are described in the Kolmozero deposit for the first time. Some inclusions contain single grains of an As-bearing mineral and unidentified Fe–Mg–K aluminosilicate. Only low-density CO_2 was identified by Raman spectroscopy in the gas bubbles of some inclusions. CO_2 is more typically observed in crystal-rich fluid inclusions that do not contain the carbonate phases zabuyelite or calcite. Rare tiny single two-phase gas-liquid inclusions containing room temperature aqueous liquid and a low-density gas bubble with, or without detectable CO_2, were observed together with crystal-rich fluid inclusions.

Thermometric studies revealed that some crystal-rich fluid inclusions were homogenised into liquid at 275–280°C. Solid phases were insensitive to heating up to 600°C.

Quartz from the quartz–muscovite veinlet contains two-phase fluid inclusions. At room temperature, fluid inclusions contain an aqueous solution and a gas bubble, and in some inclusions mineral phases. These are identified by Raman spectroscopy as calcite and nahcolite. CO_2 has been identified in some of these fluid inclusions.

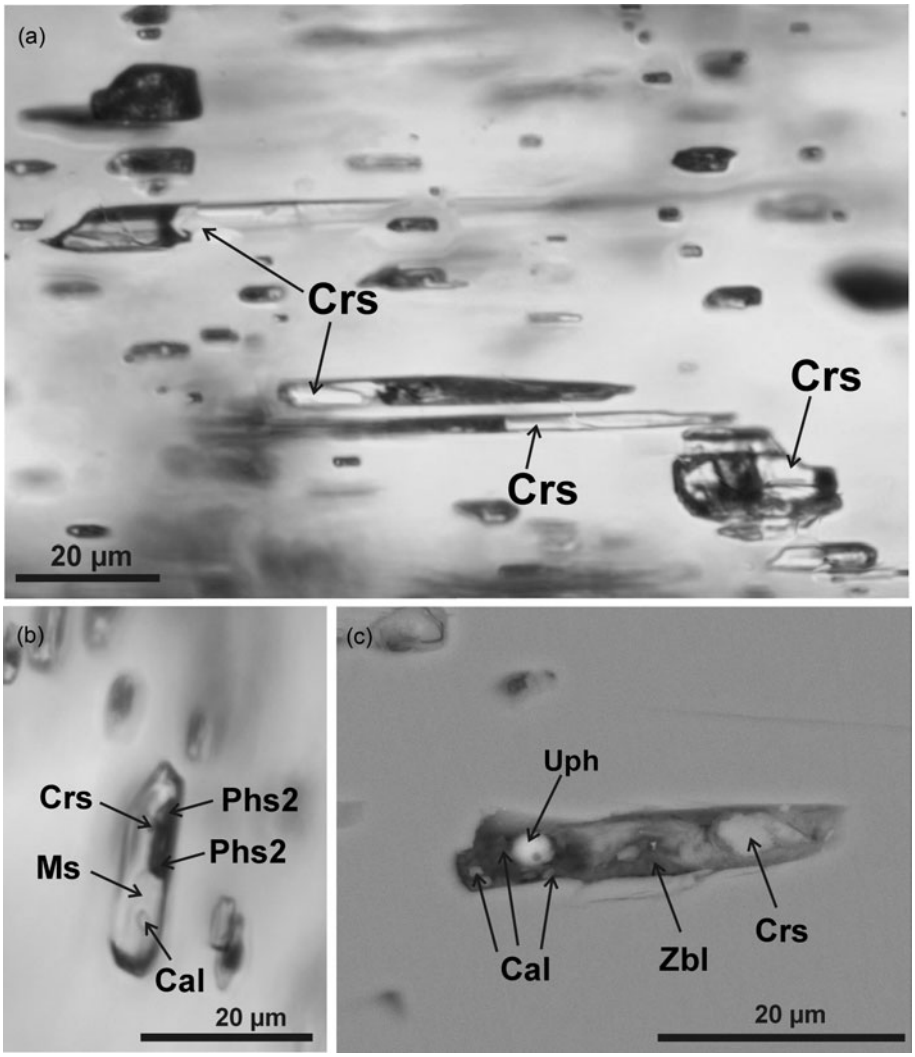

Fig. 7. Photomicrographs of crystal-rich fluid inclusions in Spd-II. (a), (b) Plane polarised light image. (c) Back-scattered electron image. Cal, calcite; Crs, cristobalite; Ms, mica; Phs2, unidentified phyllosilicate; UPh, unknown phase (Fe–Mg–K aluminosilicate); Zbl, zabuyelite.

Discussion

The most important minor elements in the spodumene from the Kolmozero albite–spodumene pegmatites are Fe and Mn. High Fe contents in the spodumene might be related to a major replacement of Al by Fe^{3+} and a subordinate replacement of Li by Fe and Mn in the spodumene structure (Deer *et al.*, 1978; Ginzburg, 1959; Bulakh *et al.*, 2014). Iron and Mn impart a green or pink tint to spodumene, respectively (Davis, 1904; Claffy, 1953; Ginzburg, 1959; Hassan and Labib, 1978; Charoy *et al.*, 1992). A high Fe content reduces the suitability of spodumene as a raw material for refractory ceramics and for use in the glass industry (Černý and Ferguson, 1972; Garrett, 2004).

High Fe contents found in the Kolmozero spodumene are typical of spodumene from rare-metal pegmatites of other regions. For example, Fe dominates over Mn, Ca, Na, K, Rb and Cs in spodumene from the rare-metal pegmatites of the Tashelga deposit in Russia (Annikova *et al.*, 2013). Iron dominates over other minor elements (Ti, Cr, V, Mn, Mg, Ca, Na, K, Sr, Zn, Nb, P, S and Ni) in the spodumene from the Kaustinen rare-metal pegmatites (Finland) (Ahtola *et al.*, 2010). Elevated Fe contents relative to those of other minor and trace elements are observed in spodumene from pegmatites of other deposits (Filip *et al.*, 2006). However, of the trace elements (Ca, Na, Fe, Mg, K, Rb, Cs and P), Na is dominant in the secondary spodumene that has extensively replaced petalite in the Tanco mine (Canada) (Černý and Ferguson, 1972; Stilling, 1998; Stilling *et al.*, 2006).

As described previously, significant variability of the Fe/Mn ratio is common for the spodumenes from the Kolmozero pegmatites. Similar variations of this ratio were also reported for granitic aplite–pegmatites from Portugal (Charoy *et al.*, 1992). These spodumenes contain Ti, Mg, Ca, Na, K, P, Rb and Cs.

Spodumene also contains, commonly, elements that are not present in its crystal structure. In the Kolmozero pegmatites, these could be due to micro-inclusions of the minerals found in crystal-rich fluid inclusions.

Crystal-rich fluid inclusions similar to those described in the Spd-II crystal from the Kolmozero lithium deposit were reported from spodumene of the Tanco (Canada), Jiajika (China) and some other pegmatites (London, 1986b, 2008; Anderson *et al.*, 2001; Thomas *et al.*, 2011; Li and Chou, 2017; Anderson, 2019). The phase composition of these crystal-rich fluid inclusions is very close to that of the Kolmozero spodumene. These crystal-rich fluid inclusions all contain gas, low-salinity aqueous fluid, and crystals of: zabuyelite; quartz/cristobalite; calcite; cookeite; mica; nahcolite; albite; and pollucite/analcime (London, 1986b, 2008; Thomas *et al.*, 2011; Li and Chou, 2017).

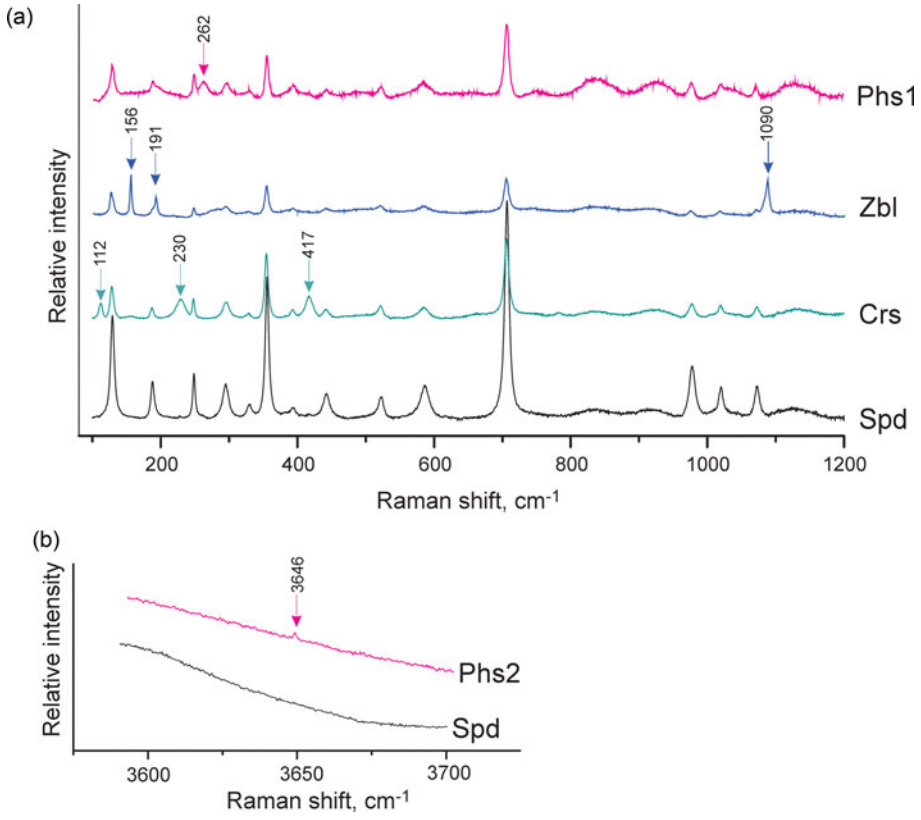

Fig. 8. Raman spectra of solid phases in spodumene-hosted crystal-rich fluid inclusions and the host Spd-II. Arrows point to the characteristic lines of the solid phases. Crs, cristobalite; Spd, host spodumene; Phs1, Phs2, unidentified phyllosilicate; Zbl, zabuyelite.

Regardless of the uniform phase composition of crystal-rich fluid inclusions, thermometric studies carried out by different researchers yielded different results. For a thermometric investigation under confining pressure conducted by London (London, 1986b, spodumene from the Tanco pegmatites) crystal-rich fluid inclusions were quenched and yielded silicate glass. Experiments by Anderson (Anderson, 2019, spodumene from Tanco) and Li and Chou (Li and Chou, 2017, spodumene from the Jiajika pegmatites) gave different results: quenched crystal-rich fluid inclusions contained aqueous fluid phase, CO_2 liquid and CO_2 vapour, but not glass. Homogenisation temperatures varied significantly from 260–400°C to 680–720°C (London, 1986b; Anderson *et al.*, 2001; Anderson, 2019; Li and Chou, 2017). These data indicate the abnormal behaviour of crystal-rich fluid inclusions upon heating. Therefore, crystal-rich fluid inclusions of the given kind are neither isochoric nor isoplethic systems and cannot be used for estimating the *P*–*T* parameters of trapping (Anderson, 2019).

We agree with Anderson's conclusion (Anderson *et al.*, 2001) that the mineral composition of the crystal-rich fluid inclusions before heating could be defined by a reaction between the trapped alkali-carbonate enriched fluid and the host spodumene. This was based on the fact that calculated bulk compositions of crystal-rich fluid inclusions had significantly higher Li concentrations in comparison with those of fluid inclusions in quartz associated with spodumene (Anderson *et al.*, 2001). As to the crystal-rich fluid inclusions in the Kolmozero spodumene, our conclusion is based on variability of the phase composition of inclusions of one fluid inclusion assemblage and the absence of CO_2 in crystal-rich fluid inclusions that contain the carbonates zabuyelite and calcite. Furthermore, according to Roedder (1984) and Heinrich and Gottschalk (1995), a reaction between the host mineral and trapped fluid is a widespread phenomenon except for cases when the host mineral is quartz.

The mechanism of formation of crystal-rich fluid inclusions through a reaction between the fluid and host spodumene is schematically based on the following reaction:

$$\mathrm{LiAlSi_2O_6 + fluid \rightarrow Li_2CO_3 + SiO_2 + LiAl_4(Si_3Al)O_{10}(OH)_8 \left(or\ KAl_3Si_4O_{10}(OH)_2\right) + H_2O + CO_2}$$

$$\text{(spodumene + fluid} \rightarrow \text{ zabuyelite + cristobalite + phyllosilicate (cookeite or mica)} + H_2O + CO_2\text{),}$$

products of which are represented by phases in crystal-rich fluid inclusions, and fluid *X* is the fluid from which the minerals formed. Carbon dioxide and aqueous solutions in crystal-rich fluid inclusions are most probably relics of the initial fluid. Thus, it can be assumed that the initial fluid was composed of $H_2O + CO_2$ + dissolved alkaline carbonates. The presence of dissolved alkaline carbonates in this fluid can be suggested from the formation of zabuyelite and calcite in the spodumene-hosted inclusions. In the course of the reaction, alumina resides in the aluminosilicate, which is represented by phyllosilicates (cookeite or mica) in the reaction above.

Thermodynamic modelling yielded a number of reactions between the indicated reagents and their products (Anderson *et al.*, 2001). For the Li_2O–Al_2O_3–SiO_2–H_2O–CO_2 system, the following reaction is proposed:

$$\mathrm{5LiAlSi_2O_6 + 2CO_2 + 4H_2O \rightarrow 2Li_2CO_3 + 7SiO_2 + LiAl_4Si_3AlO_{10}(OH)_8}$$

$$\text{(spodumene + 2CO}_2\text{ + 4H}_2\text{O} \rightarrow \text{ zabuyelite + α-quartz + cookeite)}$$

This is a subsolidus reaction proceeding at temperatures 150–200°C over a wide range of pressures. Depending on amounts of CO_2 in the trapped fluid, all Li from the reacted spodumene in crystal-rich fluid can be accommodated by zabuyelite, or, if CO_2 is relatively low, by Li-bearing aluminosilicate phases, as was illustrated by Anderson *et al.* (2001). Adding K_2O in the mineral-forming system makes other reactions possible at higher temperatures (up to *ca.* 400°C). In the spodumene-hosted inclusions reported in this study, cristobalite occurs in place of α-quartz and an unidentified phyllosilicate is postulated to be an analogue for cookeite.

Spodumene is unstable in the $LiAlSiO_4$–SiO_2–H_2O system up to temperatures of ca. 700°C at low pressure in the presence of SiO_2 (London, 1984). The occurrence of calcite and zabuyelite in the crystal-rich fluid inclusions indicates a high concentration of carbonate in aqueous solutions. Silicates and silica are easily dissolved in alkaline-carbonate aqueous solutions under hydrothermal conditions (Butuzov and Bryatov, 1957; Wilkinson *et al.*, 1996; Kotel'nikova and Kotel'nikov, 2009). It suggests that metastable spodumene is readily dissolved in a solution having the composition of the inclusions.

Fluids that were discovered in inclusions in quartz also have an aqueous-carbonate composition. Fluids in inclusions in spodumene and quartz are not coeval because the quartz veinlet cross-cuts the spodumene crystal. Although these fluids have similar compositions and are supposed to have been genetically related, i.e. quartz crystallised after spodumene under similar or even identical conditions of the pegmatite-forming system.

So, we assume that the fluid that existed during the crystallisation of mineral assemblages in the Kolmozero rare-metal pegmatite containing quartz and Spd-II had an aqueous composition with dissolved alkaline carbonates. After the entrapment this fluid reacted with the host spodumene and new solid phases: calcite; zabuyelite; cristobalite; unidentified phyllosilicate; and some others were formed in the crystal-rich fluid inclusions. Inclusions that contain silicate melt have not been found either in spodumene, or in the quartz. We suppose that some silicate melt should have been present in the pegmatite-forming system at earlier stages of formation of the Kolmozero rare-metal pegmatites and it could have been trapped by quartz and spodumene of earlier pegmatitic assemblages. However, constraining the evolution of this silicate melt and its relations to the fluids entrapped by Spd-II was outside of the scope of this work and requires further detailed study of inclusions in earlier-crystallising minerals.

Conclusions

Spodumene (Spd) is one of the main rock-forming minerals and the only primary host for lithium in rare-metal pegmatites of the Kolmozero lithium deposit, and is represented by three generations: Spd-I; Spd-II; and Spd-III (Gordienko, 1970; Morozova and Bazai, 2019). Fe, Na and Mn are the most typical impurity elements in spodumene. Spd-I is characterised by a low Fe/Mn ratio (7.1) which increases to 12.3 and 13.2 in Spd-II and Spd-III, respectively. Relatively high Fe contents in spodumene might be related to replacement of Al by Fe^{3+} together with minor replacement of Li by Fe and Mn. The increase in the Fe/Mn ratio and decrease in Mn concentration from Spd-I to Spd-III might have been related to the redistribution of Mn between spessartine, apatite, columbite-(Mn), lithiophilite and spodumene during pegmatite crystallisation. The formation of the Kolmozero pegmatite assemblages that contain Spd-II and quartz most probably occurred in a CO_2-bearing aqueous fluid with dissolved alkaline carbonates. Solid phases in the crystal-rich fluid inclusions in Spd-II include zabuyelite (Li_2CO_3), cristobalite (SiO_2), calcite and some phyllosilicates. Zabuyelite and cristobalite have not been reported previously from the Kolmozero pegmatites. These minerals have been found only in crystal-rich fluid inclusions, and are interpreted as products of reaction between the trapped fluid and host Spd-II.

Acknowledgements. The authors express their gratitude to P.A. Serov and I.A. Koval (GI KSC RAS) for the participation in field work. Mrs A.A. Merenova is thanked for translating the manuscript into English. The research has been carried out in the framework of the Scientific Research Contract of GI KSC RAS No. 0226-2019-0053, partly within the framework of State Assignment of the IGM SB RAS, and partly within the framework of State Assignment (AAAA-A18-118053090045-8) of the Geoanalitik Core Facilities Centre of the IGG UB RAS. The study was partially funded by the Russian Ministry of Higher Education and Sciences grant № 075-15-2020-802. This study has also been conducted in cooperation with and partly financed by the TD Halmek Lithium Enterprise. An authorised representative of this enterprise, Mr P.S. Galchenko participated in field work. We deeply appreciate the work of the anonymous reviewers, the editorial team of *Mineralogical Magazine* and Principal Editor, Professor R. Mitchell for their constructive criticism and correcting the English, which resulted in significant improvements to the manuscript.

References

Ahtola T., Kuusela J., Koistinen E., Seppanen H., Hatakka T. and Lohva J. (2010) *Report of Investigations on the Leviakangas Lithium Pegmatite Deposit in Kaustinen, Western Finland*. Geological Survey of Finland, archive report M 19/2323/2020/32, Kaustinen, Finland, 59 pp.

Anderson A.J. (2013) Are silicate-rich inclusions in spodumene crystallized aliquots of boundary layer melt? *Geofluids*, **13**, 460–466.

Anderson A.J. (2019) Microthermometric behavior of crystal-rich inclusions in spodumene under confining pressure. *The Canadian Mineralogist*, **57**, 853–865.

Anderson A.J., Clark A.H. and Gray S. (2001) The occurrence and origin of zabuyelite (Li_2CO_3) in spodumene-hosted fluid inclusions: implications for the internal evolution of rare-element granitic pegmatites. *The Canadian Mineralogist*, **39**, 1513–1527.

Annikova I.Yu., Vladimirov S.Z., Smirnov S.Z., Uvarov A.N., Gertner I.F. and Gavryushina O.A (2013) Geology and mineralogy of spodumene pegmatites of Mountain Shoria. *Tomsk State University Journal*, **376**, 168–174 [in Russian].

Bazarov L.Sh. (1976) Physicochemical conditions of crystallization of rare-metal granite pegmatites. Pp. 94–101 in: *Genetic Research in Mineralogy, Collection of Scientific Papers* (Yu A. Dolgov, V.P. Kostyuk and L.Sh. Bazarov, editors). USSR Academy of Sciences, Siberian branch, Institute of Geology and Geophysics, Novosibirsk [in Russian].

Bowell R.J., Lagos L., De los Hoyos C.R. and Declercq J. (2020) Classification and characteristics of natural lithium resources. *Elements*, **16**, 259–264.

Bulakh A.G., Zolotaryov A.A. and Krivovichev V.G. (2014) *Structure, Isomorphism, Formulas, and Classification of Minerals*. Saint-Petersburg University Publisher, Saint-Petersburg, Russia, 133 pp [in Russian].

Butuzov V.P. and Bryatov L.V. (1957) Study of phase equilibriums in part of the H_2O–SiO_2–Na_2CO_3 system at high temperatures and pressures. *Crystallography*, **204**, 944–947 [in Russian].

Bykhovsky L.Z. and Arkhipov N.A. (2016) Rare metal raw materials in Russia: prospects for exploration and development of mineral resource base. *Exploration and Protection of Mineral Resources*, **11**, 26–36 [in Russian].

Černý P. (1982) Anatomy and classification of granitic pegmatites. Pp. 1–39 in: *Granitic Pegmatites in Science and Industry, Short Course Handbook*. (P. Černý, editor). Mineralogical Association of Canada.

Černý P. (1991) Rare-element granitic pegmatites; Part 1, Anatomy and internal evolution of pegmatite deposits. *Geoscience Canada*, **18**, 49–67.

Černý P. (1992) Geochemical and petrogenetic features of mineralization in rare-element granitic pegmatites in the light of current research. *Applied Geochemistry*, **7**, 393–416.

Černý P. and Ercit T.S. (2005) The classification of granitic pegmatites revisited. *The Canadian Mineralogist*, **43**, 2005–2026.

Černý P. and Ferguson R.B. (1972) The Tanco pegmatite at Bernic Lake, Manitoba; IV, Petalite and spodumene relations. *The Canadian Mineralogist*, **11**, 660–678.

Chachowsky L.E. (1987) *Mineralogy, Geochemistry and Petrology of Pegmatitic Granites and Pegmatites at Red Sucker Lake and Gods Lake, Northeastern of Manitoba*. University Manitoba, Winnipeg, 157 pp.

Charoy B., Lhote F. and Dusausoy Y. (1992) The crystal chemistry of spodumene in some granitic aplite-pegmatite of northern Portugal. *The Canadian Mineralogist*, **30**, 639–651.

Claffy E.W. (1953) Composition, tenebrescence and luminescence of spodumene minerals. *American Mineralogist*, **38**, 919–931.

Daly J.S., Balagansky V.V., Timmerman M.J. and Whitehouse M.J. (2006) The Lapland–Kola orogen: Palaeoproterozoic collision and accretion of the northern Fennoscandian lithosphere. Pp. 579–597 in: *European Lithosphere Dynamics, Memoir 32* (D.G. Gee and R.A. Stephenson, editors). Geological Society, London.

Davis R.O.E. (1904) Analysis of kunzite. *American Journal of Science*, **189** (103), 1–29.

Deer W.A., Howie R.A. and Zussman J. (1978) *Rock Forming Minerals; v. 2A, Single-Chain Silicates, 2nd Edition*. London: Longman, 668 pp.

Fersman A.E. (1960) *Selected Works (VI); Pegmatites (I), Granite pegmatites*. Moscow, 745 pp [in Russian].

Filip J., Novak M. and Zboril R. (2006) Spodumene from granite pegmatites of various genetic types: crystal chemistry and OH defects concentrations. *Physics and Chemistry of Minerals*, **32**, 733–746.

Garrett D.E. (2004) *Handbook of Lithium and Natural Calcium Chloride*. Elsevier, 488 pp.

Ginzburg A.I. (1959) Spodumene and the processes of its change. *Proceedings of the Mineralogical Museum*, **9**, 12–55 [in Russian].

Glebovitsky V.A. (editor) (2005) *Early Precambrian of the Baltic shield*. Nauka, Saint-Petersburg, 711 pp [In Russian].

Gordienko V.V. (1970) *Mineralogy, Geochemistry and Genesis of Spodumene Pegmatites*. Nedra, Leningrad, 240 pp [in Russian].

Gordienko V.V. (1996) *Granite Pegmatites*. Saint Petersburg University Publishers, Saint-Petersburg, 272 pp [in Russian].

Hanski E.J. and Melezhik V.A. (2013) Litho- and chronostratigraphy of the Palaeoproterozoic Karelian formations. Pp. 39–110 in: *Reading the Archive of Earth's Oxygenation, v. 2* (V.A. Melezhik, editor). Springer. Berlin.

Hassan H. and Labib M. (1978) Induced color centers in spodumene called kunzite. *Neues Jahrbuch furMineralogie – Abhandlunger*, **134**, 104–115.

Heinrich W. and Gottschalk M. (1995) Metamorphic reactions between fluid inclusions and mineral hosts; I, Progress of the reaction calcite + quartz = wollastonite + CO_2 in natural wollastonite-hosted fluid inclusions. *Contributions to Mineralogy and Petrology*, **122**, 51–61.

Hölttä P., Balagansky V., Garde A.A., Mertanen S., Peltonen P., Slabunov A., Sorjonen-Ward P. and Whitehouse M. (2008) Archean of Greenland and Fennoscandia. *Episodes*, **31**, 13–19.

Kesler S.E., Gruber P.W., Medina P.A., Keoleian G.A., Everson M.P. and Wallington T.J. (2012) Global lithium resources: relative importance of pegmatite, brine and other deposits. *Ore Geology Reviews*, **48**, 55–69.

Kotel'nikova Z.A and Kotel'nikov A.R. (2009) Liquid separation in the presence of vapor in synthetic fluid inclusions obtained from Na_2CO_3 solutions. *Doklady Earth Sciences*, **429**, 1533–1535.

Kozlov N.E., Sorokhtin N.O., Glaznev V.N., Kozlova N.E., Ivanov A.A., Kudryashov N.M., Martynov E.V., Tyuremnov V.A., Matyushkin A.V. and Osipenko L.G. (2006) *Archean Geology of the Baltic shield*. Nauka, Saint-Petersburg, 345 pp [in Russian].

Kratz K.O. (editor) (1978) *Earth Crust of the Eastern Baltic Shield*. Nauka, Leningrad, 232 pp [In Russian].

Kudryashov N.M., Petrovsky M.N., Mokrushin A.V. and Elizarov D.V. (2013) Neoarchean sanukitoid magmatism in the Kola region: geological, petrochemical, geochronological and isotopic-geochemical data. *Petrologiya*, **21**, 351–374.

Lagache M. (1997) The Volta Grande pegmatites, Minas Gerais, Brazil: an example of rare-element granitic pegmatites exceptionally enriched in lithium and rubidium. *The Canadian Mineralogist*, **35**, 153–165.

Lahtinen R. and Huhma H. (2019) A revised geodynamic model for the Lapland-Kola orogen. *Precambrian Research*, **330**, 1–19.

Li J. and Chou I-M. (2017) Homogenization experiments of crystal-rich inclusions in spodumene from Jiajika lithium deposit, China, under elevated external pressures in a hydrothermal diamond-anvil cell. *Geofluids*, **2017**, 1–12.

London D. (1984) Experimental phase equilibria in the system $LiAlSiO_4$–SiO_2–H_2O: a petrogenetic grid for lithium-rich pegmatites. *American Mineralogist*, **69**, 995–1004.

London D. (1986a) Formation of tourmaline-rich gem pockets in miarolitic pegmatites. *American Mineralogist*, **71**, 396–405.

London D. (1986b) Magmatic-hydrothermal transition in the Tanco rare-element pegmatite: evidence from fluid inclusions and phase-equilibrium experiments. *American Mineralogist*, **71**, 376–395.

London D. (2008) *Pegmatites*. The Canadian Mineralogist, Special Publication 10, Quebec, 347 pp.

London D. (2017) Reading pegmatites: part 3 - what lithium minerals say. *Rocks & Minerals*, **92**, 143–157.

McCaffrey K.J.W., Lonergan L. and Wilkinson J.J. (1999) *Fractures, Fluid Flow and Mineralization*. Geological Society of London, London, 337 pp.

Mints M.V. (2015a) Kolmozero–Voronya belt. Pp. 39–40 in: *East European Craton: Early Precambrian History and 3D Models of Deep Crustal Structure*. (K. Condie and F.E. Harvey, editors). Geological Society of America, Special Paper 510, Boulder, Colorado.

Mints M.V. (2015b) Paleoarchean and Mesoarchean microcontinents. Pp. 19–32 in: *East European Craton: Early Precambrian History and 3D Models of Deep Crustal Structure* (K. Condie and F.E. Harvey, editors). Geological Society of America, Special Paper 510, Boulder, Colorado.

Morozova L.N. (2018) Kolmozero lithium deposit of rare metal pegmatites: new data on rare element composition (Kola Peninsula). *Litosfera*, **18**, 82–98 [in Russian].

Morozova L.N. (2019) The Kolmozero deposit: a unique Li source in the European Arctic of Russia. *IOP Conference Series: Earth and Environmental Science*, **302**, 012047, https://doi.org/10.1088/1755-1315/302/1/012047.

Morozova L.N. and Bazai A.V. (2019) Spodumene from rare-metal pegmatites of the Kolmozerskoe lithium deposit (Kola Peninsula). *Zapiski RMO*, **1**, 65–78 [in Russian].

Morozova L.N., Bayanova T.B., Bazai A.V., Lyalina L.M., Serov P.A., Borisenko E.S. and Kunakkuzin E.L. (2017) Rare metal pegmatites of the Kolmozerskoe lithium deposits of the Arctic region, the Baltic shield: new geochronological data. *Vestnik of the Kola Research Center of the Russian Academy of Sciences*, **9**, 43–52 [in Russian].

Petrov V.P., Belyaev O.A., Voloshina Z.M., Balagansky V.V., Glazunkov A.N. and Pozhilenko V.I. (1990) *Endogenous Metamorphic Regimes of the Early Precambrian (Northeastern Part of the Baltic Shield)*. Nauka, Leningrad, 184 pp [In Russian].

Roedder E. (editor)(1984) *Fluid Inclusions*. Reviews in Mineralogy 12. Mineralogical Society of America, Chantilly, Virginia, USA, 644 pp.

Rundqvist D.V. and Mitrofanov F.P. (editors) (1993) *Precambrian Geology of the USSR*. Elsevier Science, Amsterdam, 528 pp.

Stilling A. (1998) *Bulk Composition of the Tanco Pegmatites at Bernic Lake, Manitoba, Canada*. Winnipeg, Manitoba, Canada, 76 pp.

Stilling A., Černý P. and Vanstone P.J. (2006) The Tanco pegmatite at Bernic Lake, Manitoba; XVI, Zonal and bulk compositions and their petrogenetic significance. *The Canadian Mineralogist*, **44**, 599–623.

Thomas R., Davidson P. and Beurlen H. (2011) Tantalite-(Mn) from the Borborema pegmatite province, northeastern Brazil: conditions of formation and melt- and fluid-inclusion constraints on experimental studies. *Mineralium Deposita*, **46**, 749–759.

Timmerman M.J. and Daly S. (1995) Sm–Nd evidence for late Archaean crust formation in the Lapland – Kola Mobile belt, Kola Peninsula, Russia and Norway. *Precambrian Research*, **72**, 97–107.

Vetrin V.R. (1984) *Granitoids of the Murmansk Block*. Kola Branch of the Academy of Sciences of the USSR, Apatity, 123 pp [in Russian].

Vrevsky A.B. and Lvov P.A. (2016) Isotopic age and heterogeneous sources of gabbro-anorthosites from the Patchemvarek massif, Kola Peninsula. *Doklady Earth Sciences*, **469**, 716–721.

Wilkinson J.J., Nolan J. and Rankin A.H. (1996) Silicothermal fluid: a novel medium for mass transport in the lithosphere. *Geology*, **24**, 1059–1062.

Zagorsky V.E., Prokofiev V.Yu. and Kuzmina T.M. (1992) Melt inclusions in spodumene and quartz of rare metal pegmatites. *Doklady Earth Sciences*, **325**, 354–356 [in Russian].

Zhu Y.-F., Zeng Y. and Gu L. (2006) Geochemistry of the rare metal-bearing pegmatite no. 3 vein and related granites in the Keketuohai region, Altay Mountains, northwest China. *Journal of Asian Earth Sciences*, **27**, 61–77.